International Journal of Solids and Structures 45 (2008) 5556–5566

Contents lists available at ScienceDirect

International Journal of Solids and Structures

journal homepage: www.elsevier.com/locate/ijsolstr

Wedge indentation of thin films modelled by strain gradient plasticity

Per Fredriksson [a], Per-Lennart Larsson [a,*]

[a] Department of Solid Mechanics, KTH Engineering Sciences, Royal Institute of Technology, Osquars backe 1, SE-100 44 Stockholm, Sweden

ARTICLE INFO

Article history:
Received 28 March 2008
Received in revised form 16 May 2008
Available online 13 June 2008

Keywords:
Indentation
Hardness
Thin films
Size effects
Strain gradient plasticity
Finite element method
Length scales

ABSTRACT

A plane strain study of wedge indentation of a thin film on a substrate is performed. The film is modelled with the strain gradient plasticity theory by Gudmundson [Gudmundson, P., 2004. A unified treatment of strain gradient plasticity. Journal of the Mechanics and Physics of Solids 52, 1379–1406] and analysed using finite element simulations. Several trends that have been experimentally observed elsewhere are captured in the predictions of the mechanical behaviour of the thin film. Such trends include increased hardness at shallow depths due to gradient effects as well as increased hardness at larger depths due to the influence of the substrate. In between, a plateau is found which is observed to scale linearly with the material length scale parameter. It is shown that the degree of hardening of the material has a strong influence on the substrate effect, where a high hardening modulus gives a larger impact on this effect. Furthermore, pile-up deformation dominated by plasticity at small values of the internal length scale parameter is turned into sink-in deformation where plasticity is suppressed for larger values of the length scale parameter. Finally, it is demonstrated that the effect of substrate compliance has a significant effect on the hardness predictions if the effective stiffness of the substrate is of the same order as the stiffness of the film.

1. Introduction

Indentation or hardness tests have for a long time been used in order to characterize conventional engineering materials such as metals and alloys. In recent years, such tests have received increased attention due to the development of new experimental devices, such as the nanoindenter, (Pethica et al., 1983), which enable the determination of the material properties from extremely small samples. Another reason for the renewed interest in indentation testing is the fact that, for many new engineering materials, for example ceramics, a standard uniaxial test often fails to deliver reliable results. Indentation is then the only alternative for material characterization even though the interpretation of the experimental results is a fundamental difficulty in this case.

From a practical standpoint, indentation is among the most widely used methods to perform the difficult task to investigate the material properties of very thin films or coatings, and has been successfully applied for a broad range of materials when determining the strength very near the surface. Dependent on the shape of the indenter, Brinell (spherical indenter), cone, Vickers or Berkovich (sharp indenters) are the most frequently used indentation methods (geometries). In the case of thin specimens though, sharp indentation for material characterization has received a fairly wide acceptance because the large size of the spherical impression may prevent the use on small samples or in critically stressed parts where the indentation could be a potential site of failure. Thus, micro- or nanoindentation provides information about elastic and plastic deformation on a localized scale and it is particularly attractive for thin films with a typical thickness of a few micrometers or less.

* Corresponding author. Fax.: +46 8 411 2418.
E-mail address: pelle@hallf.kth.se (P.-L. Larsson).

0020-7683/$ - see front matter © 2008 Elsevier Ltd. All rights reserved.
doi:10.1016/j.ijsolstr.2008.06.001

It goes almost without saying that mechanical modelling of indentation experiments is of fundamental importance when the experimental results are to be interpreted for the purpose of, most often, material characterization. When it comes to classical elastoplastic materials, a lot of knowledge has been gained and classical results by Tabor (1951) and Johnson (1970, 1985) have been mainly confirmed but also improved by studies based on modern experimental and numerical methods, cf., e.g., Bhattacharya and Nix (1988), Laursen and Simo (1992), Biwa and Storåkers (1995), Giannakopoulos et al. (1994), Larsson et al. (1996) and Mesarovic and Fleck (1999). Accordingly, for such materials indentation can nowadays be considered as a reliable and straightforward method for determining the material properties, also when thin film/substrate systems are at issue.

However, when it comes to other types of constitutive behavior much less is known which of course is unfortunate. Indeed, the development of the nanoindenter has strongly indicated the need for a better understanding of strain gradient effects as such are very much present at, say, sub micrometer indentation. In recent years, progress concerning this issue has been achieved by, for example, Nix and Gao (1998), for sharp indentation and by Swadener et al. (2002), for spherical indentation. In the study presented by Nix and Gao (1998), a mechanism-based strain gradient plasticity theory, taken directly from the Taylor dislocation model, developed by Gao et al. (1999) and Huang et al. (2000), was used. Furthermore, experimental and numerical studies of strain gradient effects at thin film indentation have also been presented (Saha et al., 2001; Saha and Nix, 2002; Chen et al., 2004; Zhang et al., 2007). Accordingly, quite a few investigations concerning strain gradient effects at indentation have been presented even though the theoretical treatment rests on particular constitutive models. Recently, however, Gudmundson (2004) presented a unified treatment of strain gradient plasticity covering a large range of strain gradient effects in isotropic materials. The theoretical framework was subsequently implemented by Fredriksson et al. (2008) in the commercial finite element program ABAQUS (2006). It is the present intention to take advantage of the achievements presented in Fredriksson et al. (2008) in order to analyse strain gradient effects at indentation of thin films.

The strain gradient plasticity theory used in the present analysis requires additional boundary conditions for plastic strains or conjugate tractions. This implies a need for enhanced degrees of freedom in a finite element implementation, which means that writing a material routine for an existing element in a finite element program does not suffice. An element formulation that activates all required degrees of freedom is required. Consequently, the user element interface UEL in ABAQUS/Standard has been used. Constitutively, a rate-independent model has been used based on assumptions leading to a framework which displays several common features with conventional plasticity theory. The theoretical framework differs from other formulations in that the direction of plastic flow is governed by a micro-stress tensor instead of the stress deviator, which is the conventional assumption.

The problem singled out for analysis concerns wedge indentation of a thin film/substrate system assuming plane strain conditions. Indentation of thin film/substrate systems is perhaps the most common situation when sub micrometer indentation is used for material characterization. The reason for analysing plane-strain wedge indentation is first of all practical as implementation of the present constitutive model for axisymmetric or 3D-problems has not yet been completed and a corresponding analysis of such problems is left for future studies. Second, though it is indeed also of interest to be able to compare the influence of the indenter geometry on indentation results, in this case, the plane-strain results can be compared to the previously mentioned results from axisymmetric studies. In the numerical calculations, the substrate is assumed to be elastic or rigid while, as mentioned above, the film is described constitutively by the strain gradient plasticity theory. A comprehensive set of experimental data has been presented by Saha and Nix (2002) and it will be shown that the majority of the phenomena presented by these authors are qualitatively captured in the present simulations.

The most important quantities given by an indentation test are the hardness H, here and in the sequel interpreted as the mean contact pressure, the contact area A or, alternatively, the relation between the indentation force, P, and the indentation depth, h, during loading as well as during unloading. As discussed somewhat above, these quantities can be used in order to determine the constitutive properties of a material and are consequently analysed here for strain gradient plasticity. In this context, it should be emphasized that at sharp indentation, but not at for example spherical indentation, of classical elastoplastic materials the pertinent relations are independent of indentation depth as no characteristic length is present in the problem. This is in contrast to the situation in the present analysis where both strain gradient and interface effects will introduce length scales into the problem. Consequently, one of the most important tasks here is to investigate the region of validity for different solutions representing these different physical features.

To conclude then, the present investigation concerns a numerical analysis of wedge indentation of thin/film substrate systems where the material behaviour of the film is modelled by strain gradient plasticity. A few previous investigations dealing with similar problems have been presented in the literature but the present study include two new features of interest. First of all, the general theoretical framework for strain gradient plasticity presented by Gudmundson (2004) is used in the analysis and second, wedge indentation, not previously investigated in this context, is considered. Consequently, both the influence of material model and of indenter geometry can be determined by a comparison of present and previous results. In addition to this, the effect of substrate compliance is also studied in some detail.

2. Theoretical framework

The basic structure of the strain gradient plasticity theory used in the present analysis is set in Gudmundson (2004) and only the most important equations will be outlined here. Details can be found in Fredriksson et al. (2008). Conjugate stresses

that appear in the theory are, apart from the Cauchy stress σ_{ij}, the micro-stress q_{ij}, which is conjugate to the plastic strain $\epsilon^{\mathrm{p}}_{ij}$, and the moment stress m_{ijk}, which is conjugate to $\epsilon^{\mathrm{p}}_{ij,k}$. The strains are assumed to be small, such as

$$\epsilon_{ij} = \frac{1}{2}(u_{i,j} + u_{j,i}) \tag{2.1}$$

holds for displacements u_i. It has been shown by Larsson (2006) that global parameters such as load–depth relations as well as hardness can often be captured with sufficient accuracy within a small strain framework while field variables are not well reproduced at sharp indentation by such an approach.

The material response is assumed to be rate-independent and is described by the following free energy density function:

$$\Psi = \frac{1}{2}\left(D_{ijkl}\epsilon^{\mathrm{e}}_{ij}\epsilon^{\mathrm{e}}_{kl} + L^2 G \epsilon^{\mathrm{p}}_{ij,k}\epsilon^{\mathrm{p}}_{ij,k}\right). \tag{2.2}$$

The following relations can then be directly obtained:

$$\sigma_{ij} = \frac{\partial \Psi}{\partial \epsilon^{\mathrm{e}}_{ij}} = D_{ijkl}\epsilon^{\mathrm{e}}_{kl}, \tag{2.3}$$

$$m_{ijk} = \frac{\partial \Psi}{\partial \epsilon^{\mathrm{p}}_{ij,k}} = GL^2\epsilon^{\mathrm{p}}_{ij,k}, \tag{2.4}$$

where D_{ijkl} is the elastic stiffness tensor, G is the elastic shear modulus and L is a material length scale parameter. The first relation is Hooke's generalized law and the second is the simplest possible relation for energetic hardening by plastic strain gradients. Here, a more general, invariant form can be used which introduces three independent length scale parameters in Eqs. (2.2) and (2.3), see, e.g., Gudmundson (2004) and Fleck and Hutchinson (2001)). Plastic loading is governed by a flow surface f, such that

$$f = q_{\mathrm{e}} - \sigma_{\mathrm{f}} = 0 \tag{2.5}$$

is fulfilled. The effective stress $q_{\mathrm{e}} = \sqrt{3/2 q_{ij}q_{ij}}$ has been introduced. The hardening is assumed to be linear and isotropic such that the flow stress σ_{f} evolves according to

$$\sigma_{\mathrm{f}} = \sigma_{\mathrm{y}} + H_{\mathrm{f}}\epsilon^{\mathrm{p}}_{\mathrm{e}}, \tag{2.6}$$

where σ_{y} is the yield stress and H_{f} is the hardening modulus. Normality gives the increment in plastic strain as

$$\dot{\epsilon}^{\mathrm{p}}_{ij} = \dot{\lambda}\frac{\partial f}{\partial q_{ij}} = \dot{\lambda}\frac{3}{2}\frac{q_{ij}}{q_{\mathrm{e}}}, \tag{2.7}$$

where $\dot{\lambda}$ is a plastic multiplier, which can be identified with the effective plastic strain $\dot{\epsilon}^{\mathrm{p}}_{\mathrm{e}} = \sqrt{2/3\dot{\epsilon}^{\mathrm{p}}_{ij}\dot{\epsilon}^{\mathrm{p}}_{ij}}$. The consistency relation ensures that the stress state does not leave the flow surface

$$\dot{f} = \frac{\partial q_{\mathrm{e}}}{\partial q_{ij}}\dot{q}_{ij} - H_{\mathrm{f}}\dot{\lambda} = 0. \tag{2.8}$$

2.1. Principle of virtual work and finite element equations

The theoretical formulation above is used in a finite element implementation, which is based on the variational principle

$$\int_V \left(\dot{\sigma}_{ij}\delta\dot{\epsilon}_{ij} + (\dot{q}_{ij} - \dot{\sigma}_{ij})\delta\dot{\epsilon}^{\mathrm{p}}_{ij} + \dot{m}_{ijk}\delta\dot{\epsilon}^{\mathrm{p}}_{ij,k}\right)\mathrm{d}V = \int_S (\dot{T}_i\delta\dot{u}_i + \dot{M}_{ij}\delta\dot{\epsilon}^{\mathrm{p}}_{ij})\mathrm{d}S - \left\{\int_V \left(\sigma_{ij}\delta\dot{\epsilon}_{ij} + (q_{ij} - \sigma_{ij})\delta\dot{\epsilon}^{\mathrm{p}}_{ij} + m_{ijk}\delta\dot{\epsilon}^{\mathrm{p}}_{ij,k}\right)\mathrm{d}V - \int_S (T_i\delta\dot{u}_i + M_{ij}\delta\dot{\epsilon}^{\mathrm{p}}_{ij})\mathrm{d}S\right\}. \tag{2.9}$$

The bracket terms are equilibrium correction terms. The corresponding strong form is the two sets of differential equations

$$\sigma_{ij,j} = 0 \text{ in } V, \tag{2.10}$$

$$m_{ijk,k} + s_{ij} - q_{ij} = 0 \text{ in } V, \tag{2.11}$$

which have to be fulfilled together with boundary conditions for $\dot{u}_i$ or $\dot{T}_i$ and $\dot{\epsilon}^{\mathrm{p}}_{ij}$ or $\dot{M}_{ij}$, respectively. The stress deviator is denoted s_{ij}. Eq. (2.10) is the conventional equilibrium equation in the absence of body forces and Eq. (2.11) balances the higher-order stresses according to the influence by plastic strain gradients. In the absence of any gradients in plastic strain, Eq. (2.11) will give $q_{ij} = s_{ij}$, since m_{ijk} vanishes. The theory then reduces to the conventional J_2-framework.

For a numerical solution by the finite element method, a discretization technique is used that in addition to the displacements u_i, employs the plastic strains $\epsilon^{\mathrm{p}}_{ij}$ as independent variables, see Fredriksson et al. (2008). Within each element, these fields are assumed to have the following form:

$$u_i = \sum_{I=1}^{n_u} N_u^I(\xi_k) d_i^I, \tag{2.12}$$

$$\epsilon_{ij}^p = \sum_{I=1}^{n_p} N_p^I(\xi_k) e_{ij}^I. \tag{2.13}$$

Here, ξ_i denote three natural coordinates, e_{ij}^I and d_i^I are nodal values at node I, for plastic strains and displacements, respectively, and N_p^I and N_u^I are standard shape functions. The number of nodes that are utilized for the displacement field are n_u and for the plastic strain field n_p. Strains and plastic strain gradients are obtained as the derivatives

$$\epsilon_{ij} = \sum_{I=1}^{n_u} \frac{1}{2}\left(B_{uj}^I d_i^I + B_{ui}^I d_j^I\right), \tag{2.14}$$

$$\epsilon_{ij,k}^p = \sum_{I=1}^{n_p} B_{pk}^I e_{ij}^I, \tag{2.15}$$

where B_{ui}^I and B_{pi}^I are spatial derivatives of the shape functions for displacements and plastic strains, respectively. If the above discretization together with the principle of virtual work is written in matrix form, the following equation is obtained for one element:

$$\mathbf{k}_e \dot{\mathbf{p}}_e = \dot{\mathbf{f}}_e - \{\mathbf{c}_i - \mathbf{c}_e\}, \tag{2.16}$$

where

$$\mathbf{k}_e = \begin{bmatrix} \mathbf{k}_u & -\mathbf{k}_{up} \\ -\mathbf{k}_{up}^T & \mathbf{k}_p \end{bmatrix}, \quad \dot{\mathbf{f}}_e = \int_S \begin{bmatrix} \mathbf{N}_u^T \dot{\mathbf{t}}_u \\ \mathbf{N}_p^T \dot{\mathbf{t}}_p \end{bmatrix} dS \tag{2.17}$$

are the element stiffness matrix and force vector, respectively. The matrices $\mathbf{N}_u$ and $\mathbf{N}_p$ contain the shape functions and $\mathbf{t}_u$ and $\mathbf{t}_p$ the Cauchy and moment tractions, respectively. The bracket terms $\mathbf{c}_i$ and $\mathbf{c}_e$ are the equilibrium correction terms and $\dot{\mathbf{p}}_e^T = [\,\dot{\mathbf{d}}^T \quad \dot{\mathbf{e}}^T\,]$ is a vector of displacement and plastic strain degrees of freedom, respectively. Explicitly,

$$\mathbf{k}_u = \int_V \mathbf{B}_u^T \mathbf{D} \mathbf{B}_u \, dV, \tag{2.18}$$

$$\mathbf{k}_{up} = \int_V \mathbf{B}_u^T \mathbf{D} \mathbf{N}_p \, dV, \tag{2.19}$$

$$\mathbf{k}_p = \int_V \left[\mathbf{N}_p^T(\mathbf{D}_q + \mathbf{D})\mathbf{N}_p + \mathbf{B}_p^T \mathbf{D}_m \mathbf{B}_p\right] dV \tag{2.20}$$

hold, where $\mathbf{B}_u$ and $\mathbf{B}_p$ are matrices of spatial derivatives of the shape functions for displacements and plastic strains, respectively. Further,

$$\mathbf{D}_q = \frac{2}{3}\left[\frac{2}{3}(h - E_0)\mathbf{r}\mathbf{r}^T + E_0 \mathbf{I}_q\right], \tag{2.21}$$

$$\mathbf{I}_q = \mathrm{diag}[\,1 \quad 1 \quad 1 \quad 1/2 \quad 1/2 \quad 1/2\,], \tag{2.22}$$

$$\mathbf{D}_m = GL^2 \mathbf{I}_m \tag{2.23}$$

$$\mathbf{I}_m = \begin{bmatrix} \mathbf{I}_q & \mathbf{0} & \mathbf{0} \\ \mathbf{0} & \mathbf{I}_q & \mathbf{0} \\ \mathbf{0} & \mathbf{0} & \mathbf{I}_q \end{bmatrix}, \tag{2.24}$$

where $[\mathbf{r}]_{ij} = (3/2)(q_{ij}/q_e)$ and $\mathbf{D}$ is the elasticity matrix. The parameter E_0 is a penalty parameter that is required in order for the consistency condition equation (2.8) to be fulfilled, see Fredriksson et al. (2008) for details.

3. Problem formulation and numerical implementation

3.1. Problem

A film/substrate system with width and thickness $100t$ and film thickness t is indented by a wedge, see Fig. 1. The wedge is assumed to be rigid and frictionless contact is assumed as frictional effects are known to be small when global indentation properties are concerned, cf., e.g., Carlsson et al. (2000). The tip angle is $\alpha = 20^\circ$, which corresponds approximately to a Vickers indenter. Depending on the mechanical behaviour, the deformation may result in material being piled-up or sinked-in outside the contact edge. Pile-up or sink-in is not known à priori, but is an outcome of the resulting deformation field. As a consequence, the actual contact depth will differ from the indentation depth as well as the actual contact area A (per unit length) from the nominal contact area A_n (per unit length). For pile-up, $h_c/h > 1$ and

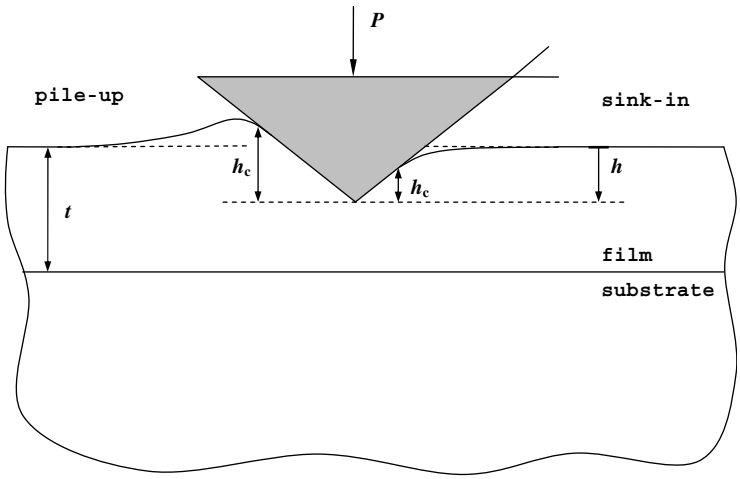

Fig. 1. Problem setup consisting of a thin film on an elastic substrate being indented by a rigid wedge at frictionless contact. The indentation depth is denoted h, the film thickness t, the force P (per unit length) and α is the tip angle. The actual contact depth h_c, which is a result of the deformation field, may exceed the indentation depth (pile-up) or fall below (sink-in).

$A/A_n > 1$ hold and sink-in is equivalent to $h_c/h < 1$ and $A/A_n < 1$. It should be noted in passing that the ratio h_c/h (and A/A_n) is constant at indentation of a half-plane of homogeneous material where the constitutive behaviour is described by J_2-plasticity. This is due to the fact that the problem is self-similar with no characteristic length present. In such a situation then, this ratio can be used for material characterization. In theory, this could be the case also at indentation of strain gradient materials even though the difficulties involved are then substantial in particular when thin film/substrate systems are at issue. Some guidance however, as regards for example the length scale parameter can definitely be given by studying the value on h_c/h and A/A_n.

The hardness is defined as the average contact pressure, $H = P/A$, which according to Fig. 1 gives

$$H = \frac{P \tan \alpha}{2h_c}. \tag{3.1}$$

3.2. Implementation

The film is constitutively modelled using strain gradient theory and the substrate is assumed to be governed by isotropic, linear elasticity. Numerical results have been generated with the finite element code (ABAQUS, 2006). The theory has been implemented in the general element interface UEL and is used in conjunction with the existing contact routine in ABAQUS. Node-to-surface contact is used which is enforced using the augmented Lagrange method. The boundary conditions are given by the symmetry conditions as well as the higher-order boundary condition $\epsilon^p_{ij} = 0$ at the film/substrate interface, which is non-conventional. The latter is motivated by the constrained dislocation movement that exists at an interface that separates a film and a substrate.

The finite element used in the simulations is a 4-noded isoparametric, bi-linear, quadrilateral plane strain element. The element interpolates plastic strains $(\epsilon^p_{11}, \epsilon^p_{22}, \epsilon^p_{12})$ in addition to displacements (u_1, u_2), see Eq. (2.12) and (2.13). Hence, five degrees of freedom is used for each node. In the finite element model, element density is high in the vicinity of the indenter and in a region in the substrate close to the interface between the film and the substrate. In total, 4935 elements and 5057 nodes have been used in the model of which 3458 elements and 3618 nodes belong to the film, see Fig. 2. The total number of degrees of freedom is 25,566. The implementation has been verified against analytical solutions as well as the elastic and local plasticity solution (Fredriksson et al., 2008). Mesh convergence, in relation to the contact problem, was also studied extensively and it was found that a ratio, between the element length in the contact region and the film thickness, being 0.02 was sufficient in order to obtain high accuracy results. Decreasing the element size further by a factor of 4 changes the hardness values by an amount of 0.8%. The thickness and width of the film/substrate system, $100t$, proved to be sufficient for strain gradients to vanish. Hence, the outer boundaries of the model are representative of a half-plane with infinite boundary conditions. In order to further check the reliability of the numerics involved in this investigation the behaviour of the load P, and the contact area A, at progressing indentation was studied. When homogeneous materials governed by J_2-plasticity are at issue it is easily shown by dimensional considerations that these quantities should be linear functions of the indentation depth h. This feature was captured with very good accuracy in our FEM-calculations giving further confidence in the reliability of the presently used numerical scheme.

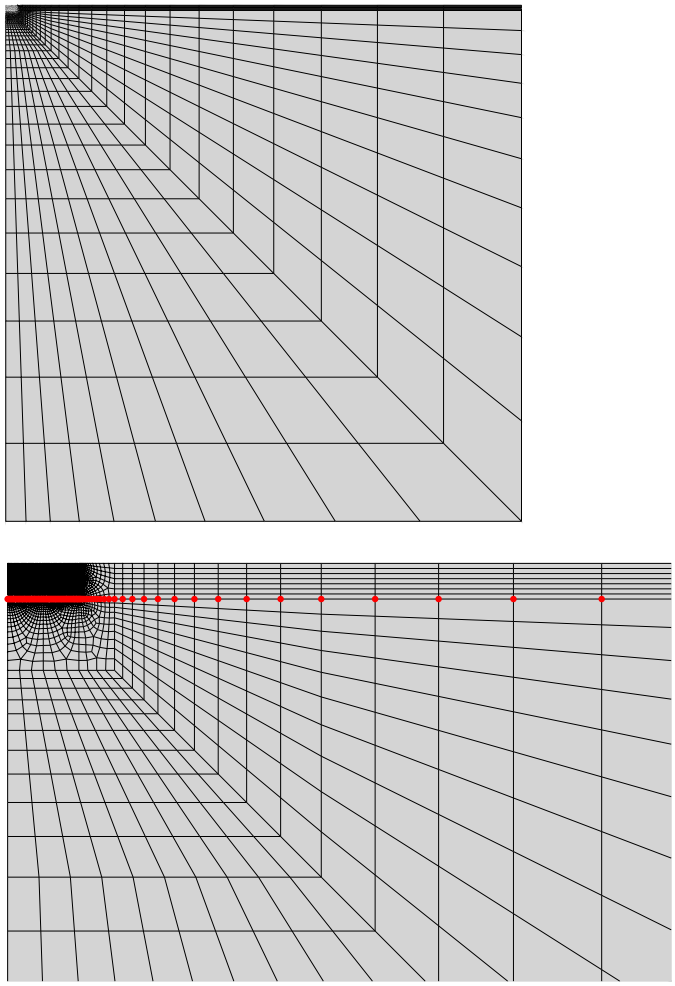

Fig. 2. Finite element model of the film/substrate system. The entire model (top) and a close-up of the contact area in the film (bottom) is shown and nodes at the interface are highlighted.

4. Results

4.1. Influence of the material length scale parameter

In Sections 4.1 and 4.2, situations will be analysed where the film is much softer than the substrate. In fact, the substrate will be assumed to be rigid such that the deformation is neglected. Hence, the substrate is removed from the simulations and replaced by clamped boundary conditions. First, the influence of the material length scale parameter on the response of the film will be studied. The parameters used are $E/\sigma_y = 400$, $E/H_f = 40$, $\nu = 0.3$. The penalty parameter is given by $E_0 = 100H_f$. In Fig. 3(a), load–depth relations are shown and in Fig. 3(b) the hardness is shown for different depths of indentation. The conventional J_2-solution (equivalent to $L \to 0$) is included. It can be observed that initially, the hardness decreases with increasing depth. The hardness does, however, not approach the value predicted by the local theory, but it reaches a plateau, H_{plateau}, after which it increases. This behaviour is not observed for bulk materials, where the hardness for larger depths of indentation saturates at a constant value. Consequently, this effect is solely due to the presence of the substrate. Experimental observations have been reported by Saha and Nix (2002), which also clearly display this type of behaviour. Numerical results from simulations by Saha et al. (2001) and Chen et al. (2004) have also predicted this behaviour. Further, the location of the plateau is found to scale with the length scale parameter L, which is illustrated in Fig. 4 for two levels of hardening of the material, $E/H_f = 40, 20$. The quantity H_{plateau} is the local minima that define the plateau of the predicted hardness. It can be seen that the scaling is linear for different values of the length scale parameter and H_{plateau} is shifted as the hardening modulus increases.

The length scale parameter has a profound influence on the deformation field. This is obvious since $L \in]0, \infty[$ generates theoretical predictions which falls between the local J_2-solution and the elastic solution. The elastic solution, equivalent

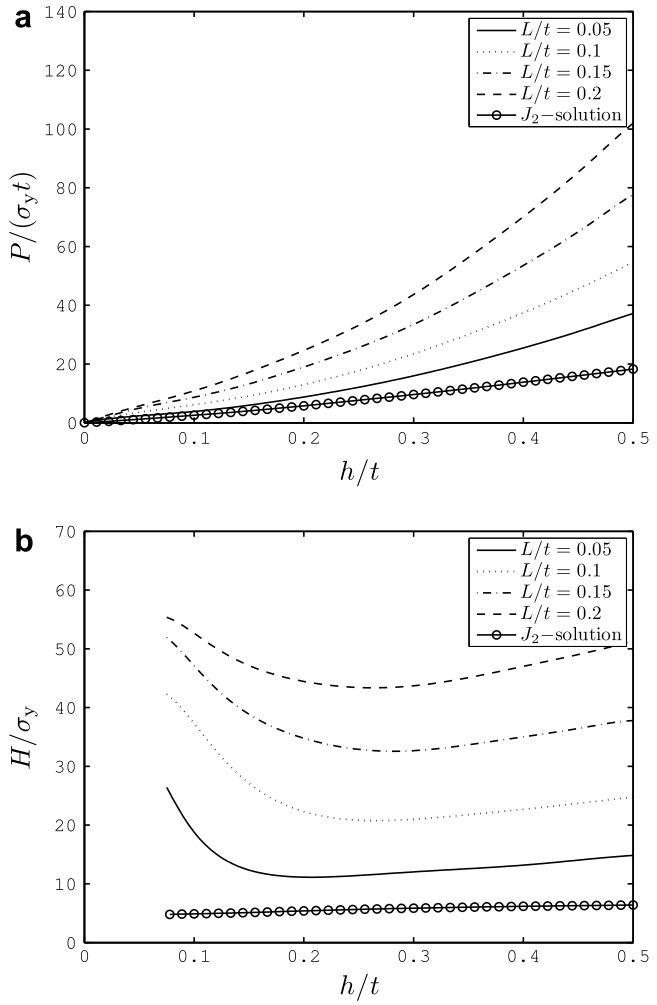

Fig. 3. Relations for different values of the internal length scale parameter. The hardening is defined by $E/H_f = 40$. (a) Load–depth relation and (b) hardness–depth relation.

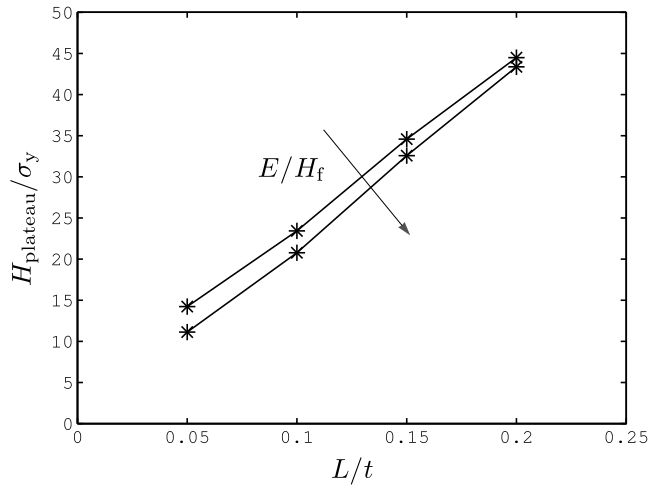

Fig. 4. Plateau values of hardness vs. material length scale parameter. Two values of the hardening modulus of the material has been used, $E/H_f = 40, 20$.

to $L \to \infty$, involves only sink-in behaviour at the indenter. As the length scale decreases, plastic activity increases in the film. Since plastic deformation is incompressible, this means less and less relative volume change. The material is then pushed upwards and the actual contact area increases. The largest contact area, predicted by the conventional J_2-theory, is approached by the smaller length scales. Consequently, at some intermediate length scale, sink-in behaviour is turned into pile-up behaviour, which is shown through the ratio h_c/h at $h = 0.5t$ in Fig. 5. The transition length scale is denoted L^*. This behaviour is important in the case of material characterization of thin films and especially for very thin films on hard substrates, where the pile-up effect is significant. Many standard indentation procedures do not account for pile-up, which means that an overestimation is obtained in the hardness calculations. It should be emphasized that this effect is present for all types of material behaviour and is not restricted to strain gradient plasticity. In addition, it should be mentioned that sink-in deformation also can cause problems when experimental results are to be interpreted as in such a case the true contact area is difficult to determine. Numerical results as presented here can then serve as a useful guidance.

4.2. Effect of the hardening modulus

In Fig. 6(a) and (b), relations are shown for different hardening moduli, H_f, of the material. It can be seen that the hardness raising effect of the substrate is amplified as the hardening modulus increases in Fig. 6(b). This originates from the reduced plastic relaxation under the indenter. The influence on the stress field from the indenter is increased as the plastic deformation is decreased for increasing values of L. The location of the plateau is constant for different values of H_f, as well as the rate of the initial decrease in hardness. One can expect that materials that display a lower degree of hardening, for which the substrate raising effect is not visible in the range of depths presented here, the substrate would influence the hardness at larger depths of indentation, $h > 0.5t$. In order to capture such behaviour with the present strain gradient model, a finite strain framework is recommended, and most probably needed.

4.3. Influence of substrate compliance

The deformation of the substrate is now accounted for. Depending on the level of this effect, the measured hardness of thin films may be more or less affected at particular values of h/t. The ratio $\bar{E} = E_{\text{substrate}}/E_{\text{film}}$ characterizes the elastic compliance of the substrate relative to the compliance of the film. The film is characterized by the length scale parameter $L/t = 0.05$ and the hardening modulus is $E/H_f = 20$, which are held constant for all cases in the model. It will be assumed that the substrate deforms elastically at all time. In Fig. 7(a) and 7(b), the film behaviour is shown for different values of $\bar{E}$. If the substrate is stiff compared to the film, which corresponds to a large $\bar{E}$, it can be seen that the substrate compliance effect is negligible on the global parameters load and hardness. Qualitatively, this type of behaviour has also been captured in simulations by Saha et al. (2001) for the case of a soft film on a hard substrate (deformable but stiff). However, when the substrate stiffness is of the same order as the film stiffness, $\bar{E} = 1$, these parameters are indeed affected. The most pronounced effect can be observed for larger depths of indentation when the hardness increases due to the presence of the substrate. For a compliant substrate, $\bar{E} = 0.5$, the hardness plateau seems to extend such that the hardness increases only slightly due to the substrate, at the present depths of indentation. If the substrate is very compliant, $\bar{E} = 0.1$, the plateau is never reached for $h = 0.5t$. The explanation is that the whole film/substrate system is bowing out due to the compliant substrate which is more susceptible to deformation. An identical behaviour has been observed by Zhang et al. (2007) for

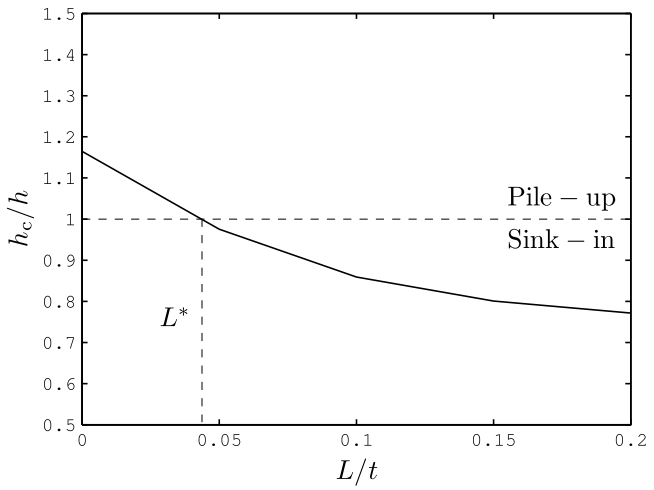

Fig. 5. Ratio of actual contact depth and nominal contact depth as influenced by the material length scale parameter at $h = 0.5t$, which indicates pile-up or sink-in. The transition length scale parameter is denoted L^* and $E/H_f = 40$ is used.

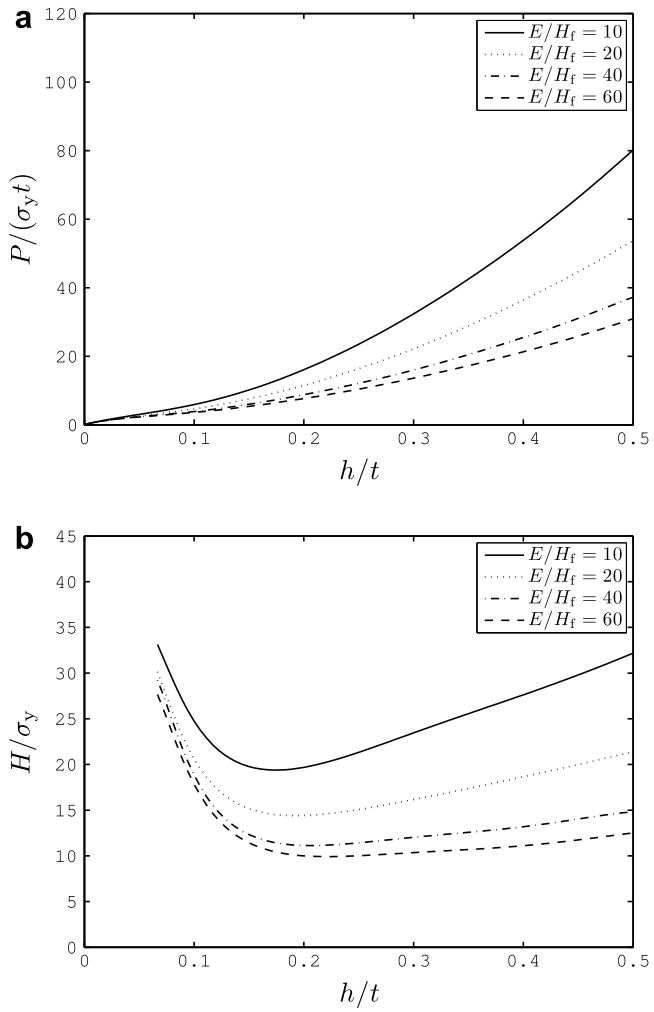

Fig. 6. Relations for materials with different hardening modulus H_f. The material length scale parameter is $L/t = 0.05$. (a) Load–depth relation and (b) hardness–depth relation.

the indentation of a hard tungsten film on a soft, plastically deforming aluminum substrate. The hardness prediction of the film is affected in the same way although the substrate deforms beyond elasticity in their analysis. It is also believed that in simulations, when indentation is performed with a monotonic load and the contact area is obtained directly from the analysis, this substrate bending effect can be captured with the parameter $\bar{E}$ only. Quantitative estimates is however not possible with the present linear elastic model for the substrate, since the aluminum substrate deforms elastic-plastically, which corresponds to a non-linearly evolving $\bar{E}$. It should be further mentioned that in experiments, the hardness is calculated based on values of the contact stiffness $S = \mathrm{d}P/\mathrm{d}h$, which is strongly affected by $\bar{E}$ as well as the plastic properties of the substrate.

The assumption of a purely elastic substrate is used throughout the analysis. By studying the effective stress values in the substrate close to the interface it is found that this is a very good assumption for soft films but worse for hard films on a soft substrate. This feature is also enhanced for increased values on the internal length scale parameters and is in good agreement with results from previous investigations by Saha et al. (2001) and Zhang et al. (2007). However, the region of high stresses close to the interface is relatively small and it is therefore believed that the assumptions of a purely elastic substrate does not significantly affect the values of the global indentation parameters presented here. In addition, it should be emphasized once again that for a more detailed study of the field variables a finite strain analysis of the problem is most certainly needed.

5. Discussion

Indentation testing is one of the most easily available methods for extracting elastic and plastic material properties, especially in the design and testing of thin films. Experimentally, tests for thin films are far more demanding than indentation testing of bulk materials. There are several difficulties, both when extracting plastic and elastic properties, that one is faced

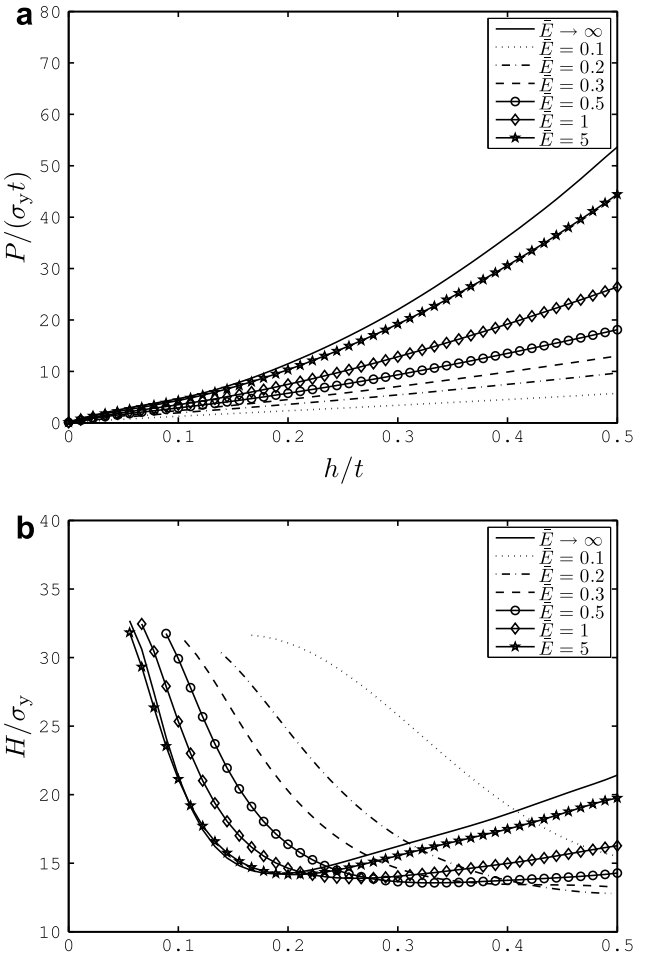

Fig. 7. Illustration of the influence of substrate compliance on the predicted film response at different depths of indentation. The material length scale parameter is $L/t = 0.05$ and the hardening modulus is given by $E/H_f = 20$. (a) Load–depth relation and (b) hardness–depth relation.

with. The influence of substrate compliance, in this study reflected by $\bar{E} = E_{\text{substrate}}/E_{\text{film}}$, on the determination of the elastic modulus is even larger than its effect on the determination of hardness. An overestimation is obtained if $\bar{E} > 1$ and an underestimation if $\bar{E} < 1$. Hence, there are notable challenges that complicate testing of thin films by nanoindentation as a tool for material characterization. When it comes to the solution of indentation problems as a way of distinguishing between different strain gradient plasticity theories, one is faced with further challenges. Large strains are always involved locally in contact problems. It sets requirements on reliable stress–strain data at large strains, as well as the methods used when solving the boundary value problem. Nevertheless, indentation testing is one of few available methods for material characterization which motivates further work on both modelling and experiments.

The small strain approximation used sets limitations in the present analysis. For depths of indentation on the order of $h = 0.5t$ the strains are significant underneath the indenter. Results are difficult to obtain for larger depths of indentation because strains are too large and elements have to be remeshed. In the results presented, an increase in hardness due to the substrate has been observed at $h < 0.5t$, which is earlier than reported in experiments in the literature, see, e.g., Saha and Nix (2002). Several parameters affect the location of this plateau, e.g., the length scale parameter, substrate compliance and higher-order boundary conditions. The assumptions of $\bar{E} \to \infty$ has a strong influence on the location of the hardness plateau. Relaxing this condition delays the plateau to larger depths, which also can be seen in Fig. 7(b). This assumption, however, makes the analysis systematic and clarifies the results significantly. It is interesting to note however that the discrete dislocation simulations by Balint et al. (2006), although in a two-dimensional dislocation environment, predict plateau loci at $h = 0.04t,\ 0.1t$ for wedge angles $\alpha = 5^\circ,\ 10^\circ$, respectively. This is at even shallower depths than the present predictions. Furthermore, it should be mentioned that the hardness values reported in Section 4 is not shown for small values of h. This is due to the discreteness of the model, i.e., when only a few elements are in contact, reliable hardness values are not obtained, and therefore not shown. In a finite strain framework, a larger range of results are possible and, hence, an interesting next step would be to study local parameters such as contact pressure and plastic strain distributions for different length scale parameters and hardening moduli.

6. Conclusions

The strain gradient plasticity theory based on Gudmundson (2004) and applied by Fredriksson et al. (2008) has been used in a contact analysis of plane strain wedge indentation of a thin film on an elastic substrate. Numerical results have been generated by the finite element method and focus has been directed towards global parameters such as indentation load and estimated hardness values for different depths of indentation. Initially, the deformation of the substrate was neglected in order to perform a more clear and systematic analysis. The influence of the material length scale parameter as well as the hardening modulus have been investigated. Subsequently, the impact of substrate compliance has been analysed and observations in experiments as well as earlier simulations have been captured. The following conclusions can be drawn:

- If the deformation of the substrate is neglected, the following trends can be observed in the hardness predictions: (I) For small depths of indentation, the hardness decreases as the depth increases. (II) At larger depths, a plateau is reached which often does not approach the value predicted by conventional plasticity theory. (III) At large depths, the hardness increases due to the presence of the substrate. All the above phenomena have been observed in experiments, e.g., by Saha and Nix (2002). Simulations by Saha et al. (2001), using a different constitutive model, have also found qualitatively the same behaviour. In addition, the plateau values are here found to scale linearly with the material length scale parameter.
- The hardening modulus of the material strongly affects the hardness raising effect of the substrate. A material which is more prone to hardening will display a larger increase in hardness due to substrate effects, than a material with a lower degree of hardening.
- The substrate compliance strongly affects the hardness predictions, in particular the location of the plateau. The film/substrate system then gradually starts to bow out, which will affect the calculated hardness values as well as the actual measured penetration of the indenter into the film. Simulations by Zhang et al. (2007) have reported similar behaviour for a hard film on a soft substrate, although modelled with other constitutive models.
- Depending on the deformation field, the material at the indenter may be piled-up or sinked-in. The material length scale parameter has a large impact on the amount of plastic deformation in the film such that a transition length scale L^* has been found that separates these two deformation modes.

Finally, it should be emphasized, as already mentioned above, that most of the conclusions listed above are in good agreement with previous numerical studies of similar indentation problems using different constitutive descriptions of strain gradient plasticity and other sharp indenter geometries. Consequently, it can be concluded from the present investigation that at least the qualitative behaviour (of global indentation variables) are not very sensitive, at indentation of thin film/substrate systems, of these two features.

Acknowledgment

The author gratefully acknowledge the financial support from the Swedish Research Council under contract 621-2001-2643.

References

ABAQUS/Standard 6.7, 2006. Abaqus Users' Manual. (www.simulia.com).
Balint, D.S., Deshpande, V.S., Needleman, A., Van der Giessen, E., 2006. Discrete dislocation plasticity analysis of wedge indentation of films. J. Mech. Phys. Solids 54, 2281–2303.
Bhattacharya, A.K., Nix, W.D., 1988. Finite element analysis of cone indentation. Int. J. Solids Struct. 27, 1047–1058.
Biwa, S., Storåkers, B., 1995. An analysis of fully plastic brinell indentation. J. Mech. Phys. Solids 43, 1303–1333.
Carlsson, S., Biwa, S., Larsson, P.-L., 2000. On frictional effects at inelastic contact between spherical bodies. Int. J. Mech. Sci. 42, 107–128.
Chen, S., Liu, L., Wang, T., 2004. Size dependent nanoindentation of a soft film on a hard substrate. Acta Mater. 52, 1089–1095.
Fleck, N.A., Hutchinson, J.W., 2001. A reformulation of strain gradient plasticity. J. Mech. Phys. Solids 49, 2245–2271.
Fredriksson, P., Gudmundson, P., Mikkelsen, L.P., 2008. Finite element implementation and numerical issues of strain gradient plasticity with application to metal matrix composites. Technical report No. 449, Department of Solid Mechanics, Royal Institute of Technology, Stockholm.
Gao, H., Huang, Y., Nix, W.D., Hutchinson, J.W., 1999. Mechanism-based strain gradient plasticity – I. Theory. J. Mech. Phys. Solids 47, 1239–1263.
Giannakopoulos, A.E., Larsson, P.-L., Vestergaard, R., 1994. Analysis of Vickers indentation. Int. J. Solids Struct. 31, 2679–2708.
Gudmundson, P., 2004. A unified treatment of strain gradient plasticity. J. Mech. Phys. Solids 52, 1379–1406.
Huang, Y., Gao, H., Nix, W.D., Hutchinson, J.W., 2000. Mechanism-based strain gradient plasticity – II Analysis. J. Mech. Phys. Solids 48, 99–128.
Johnson, K.L., 1970. The correlation of indentation experiments. J. Mech. Phys. Solids 18, 115–126.
Johnson, K.L., 1985. Contact Mechanics. Cambridge University Press, Cambridge.
Larsson, P.-L., 2006. Modelling of sharp indentation experiments: some fundamental issues. Philos. Mag. 86, 5155–5177.
Larsson, P.-L., Söderlund, E., Giannakopoulos, A.E., Rowcliffe, D.J., Vestergaard, R., 1996. Analysis of Berkovich indentation. Int. J. Solids Struct. 33, 221–248.
Laursen, T.A., Simo, J.C., 1992. A study of the mechanics of microindentation using finite elements. J. Mater. Res. 7, 618.
Mesarovic, S.D., N.A., Fleck, 1999. Spherical indentation of elastic–plastic solids. Proc. Roy. Soc. London A 455, 2707–2728.
Nix, W.D., Gao, H., 1998. Indentation size effects in crystalline materials: A law for strain gradient plasticity. J. Mech. Phys. Solids 46, 411–425.
Pethica, J.B., Hutchings, R., Oliver, W.C., 1983. Hardness measurement at penetration depths as small as 20 nm. Philos. Mag. A 48, 593–606.
Saha, R., Nix, W.D., 2002. Effects of the substrate on the determination of thin film mechanical properties by nanoindentation. Acta Mater. 50, 23–38.
Saha, R., Xue, Z., Huang, Y., Nix, W.D., 2001. Indentation of a soft metal film on a hard substrate: strain gradient hardening effects. J. Mech. Phys. Solids 49, 1997–2014.
Swadener, J.G., George, E.P., Pharr, G.M., 2002. The correlation of the indentation size effect measured with indenters of various shapes. J. Mech. Phys. Solids 50, 681–694.
Tabor, D., 1951. Hardness of metals. Oxford University Press, Oxford.
Zhang, F., Saha, R., Huang, Y., Nix, W.D., Hwang, K.C., Qu, S., Li, M., 2007. Indentation of a hard film on a soft substrate: strain gradient hardening effects. Int. J. Plast. 23, 25–43.